BB

GSI

GSI-Preprint-97-61
Oktober 1997

INVARIANT MASS SPECTRUM AND α - n CORRELATION FUNCTION STUDIED IN THE FRAGMENTATION OF ^{6}He ON A CARBON TARGET

D. Aleksandrov, T. Aumann, L. Axelsson, T. Baumann, M.J.G. Borge, L.V. Chulkov, J. Cub, W. Dostal, B. Eberlein, Th.W. Elze, H. Emling, H. Geissel, V.Z. Goldberg, M. Golovkov, A. Grünschloß, M. Hellström, J. Holeczek, R. Holzmann, B. Jonson, A.A. Korshenninikov, J.V. Kratz, G. Kraus, R. Kulessa, Y. Leifels, A. Leistenschneider, T. Leth, I. Mukha, G. Münzenberg, F. Nickel, T. Nilsson, G. Nyman, B. Petersen, M. Pfützner, A. Richter, K. Riisager, C. Scheidenberger, G. Schrieder, W. Schwab, H. Simon, M. Smedberg, M. Steiner, J. Stroth, A. Surowiec, T. Suzuki, O. Tengblad, M. V. Zhukov

(To be published in Nucl. Phys. A)

Gesellschaft für Schwerionenforschung mbH
Planckstraße 1 • D-64291 Darmstadt • Germany
Postfach 11 05 52 • D-64220 Darmstadt • Germany

Invariant mass spectrum and $\alpha - n$ correlation function studied in the fragmentation of ^{6}He on a carbon target

D. Aleksandrov[1], T. Aumann[2], L. Axelsson[3], T. Baumann[4], M.J.G. Borge[5], L.V. Chulkov[1], J. Cub[4,6], W. Dostal[2], B. Eberlein[2], Th.W. Elze[7], H. Emling[4], H. Geissel[4], V.Z. Goldberg[1], M. Golovkov[1], A. Grünschloß[7], M. Hellström[4], J. Holeczek[4,8], R. Holzmann[4], B. Jonson[3], A.A. Korshenninikov[9], J.V. Kratz[2], G. Kraus[4], R. Kulessa[10], Y. Leifels[4], A. Leistenschneider[7], T. Leth[11], I. Mukha [1,11], G. Münzenberg[4], F. Nickel[4],T. Nilsson[3], G. Nyman[3], B. Petersen[11], M. Pfützner[4], A. Richter[6], K. Riisager[11], C. Scheidenberger[4], G. Schrieder[6], W. Schwab[4], H. Simon[6], M.H. Smedberg[3], M. Steiner[12], J. Stroth[7], A. Surowiec[4,8], T. Suzuki[9], O. Tengblad[5] and M.V. Zhukov[3]

October 9, 1997

1. Kurchatov Institute, 123182 Moscow, Russia
2. Institut für Kernchemie, Johannes Gutenberg-Universität, D–55099 Mainz, Germany
3. Fysiska Institutionen, Chalmers Tekniska Högskola and Göteborgs Universitet, S–412 96 Göteborg, Sweden
4. Gesellschaft für Schwerionenforschung (GSI), D–64291 Darmstadt, Germany
5. Instituto Estructura de la Materia, CSIC, E–28006 Madrid, Spain
6. Institut für Kernphysik, Technische Universität, D–64289 Darmstadt, Germany
7. Institut für Kernphysik, Johann-Wolfgang-Goethe-Universität, D–60486 Frankfurt, Germany
8. Instytut Fizyki, Uniwersytet Śląski, PL-40-007 Katowice, Poland
9. RIKEN, 2-1 Hirosawa, Wako, Saitama 351-01, Japan
10. Instytut Fizyki, Uniwersytet Jagielloński, PL–30-059 Kraków, Poland
11. Institut for Fysik og Astronomi, Aarhus Universitet, DK–8000 Aarhus C, Denmark
12. Michigan State University, East Lansing, MI 48824-1321, USA

Abstract

Momentum distributions and invariant mass spectra from the breakup of ^{6}He ions with an energy of 240 MeV/u interacting with a carbon target have been studied. The data were used to extract information about the reaction mechanism which is influenced by the structure of ^{6}He. It is found that the dominant reaction mechanism is a two-step process: knock out of one neutron followed by the decay of the ^{5}He resonance. The shape of the $(\alpha + n)$ two-body invariant mass spectrum is interpreted as mainly reflecting the ^{5}He ground state which is a J^π=3/2$^-$ resonance. However, no evidence for correlations between α particles and neutrons is observed in the momentum widths of the distributions. It is demonstrated that a combined analysis of the two-body invariant mass spectrum and an appropriate correlation function may be used to determine the properties of the intermediate resonance.

PACS numbers: 25.60.-t, 25.70Ef, 27.20+n

Keywords: secondary radioactive beams, exotic nuclei, halo nuclei, ^{6}He, ^{5}He, momentum distributions, invariant mass spectra, fragmentation mechanism, breakup reactions

1 Introduction

The occurrence of nuclear halos is one of the most intriguing features observed for light exotic nuclei. An intense scientific activity, both experimental and theoretical, has over the last decade been developed in order to understand the basic structure of the halo states [1, 2, 3]. Special attention has been paid to nuclei showing a halo state consisting of two neutrons. These two-neutron halo nuclei are three-body systems with no bound binary sub-system and are sometimes referred to as Borromean nuclei [3].

The lightest Borromean nucleus is ^{6}He. With its two-neutron separation energy of 973 keV, it shows evidence for a halo structure [4, 5]. This nucleus has not been investigated as carefully as ^{11}Li where a large amount of data exists [1, 2]. There are, however, two essential advantages with ^{6}He: the basic $\alpha - n$ and $n - n$ interactions are well known and good wave functions from different microscopic three-body models are available [6, 7, 8, 9, 10]. This means that it becomes much simpler to make an unambiguous analysis of the influence of the reaction mechanism [11] which may be used in the interpretations of results from other halo nuclei. The ^{6}He fragmentation at high energies (400 MeV/u and 800 MeV/u) has earlier been studied experimentally [12, 13]. Transverse momentum distributions of both α-particles and neutrons were analysed [14].

In this paper, we present new experimental data for fragmentation of a 240 MeV/u ^{6}He beam in a carbon target. The complete information of the momenta of the incoming beam and the outgoing α-particles and neutrons makes a combined analysis of the $\alpha - n$ invariant mass spectrum and the correlation function possible.

2 Experimental set-up

The present experiment was performed at GSI in Darmstadt, where a secondary beam of ^{6}He (240 MeV/u) was produced in a 8 g/cm^2 beryllium production target from a primary beam of ^{18}O with an energy of 340 MeV/u. The ^{6}He nuclei were separated out from the primary reaction products using the fragment separator FRS [15]. After separation, the beam was transferred to a cave with the experimental set-up.

The experimental method is very similar to that of a measurement described earlier [16, 17, 18], and here we just summarize the main features relevant for the analysis presented in this paper.

The direction of the incoming beam was defined by a position-sensitive multi-wire proportional chamber (MWPC), placed at the entrance of the cave, together with a MWPC placed close to the 1.87 g/cm^2 carbon target (angular resolution σ_θ= 0.14 mrad). The angular distribution of charged fragments was measured by a third MWPC with a resolution σ_θ= 3.2 mrad. The charged fragments were deflected and analysed in the dipole magnet ALADIN in conjunction with position-sensitive multiwire drift chambers and a plastic wall (TOF). The time of flight between a scintillator placed at the entrance of the cave and the TOF was registered. Further, the energy loss in the TOF scintillator gave the charge of the detected fragment. Such information was also available from two thin silicon pin-diode detectors placed close to the reaction target both downstream and upstream. The neutrons were detected in the large area neutron detector (LAND) [18] with an efficiency of 85±2 %, angular resolution of 7 mrad and time of flight resolution of about 0.5 ns (FWHM).

The event class considered in this paper consists of coincidences between an α -particle and a neutron. This condition means that the α -particle core in ^{6}He has had no substantial interaction with the target which implies that the selected events originated in peripheral collisions. In order to have a basis for a discussion of the experimental data, we first describe the model used for the reaction mechanism.

3 Sequential fragmentation of ^{6}He

Korsheninnikov and Kobayashi [14] have studied ^{6}He fragmentation and found that the α-n final state interaction dominates the experimentally observed distributions where neutrons are registered in coincidence with an α-particle. Recent calculations [19] based on microscopic models have confirmed this conclusion. The ground state of ^{5}He is a comparatively long lived resonance (Γ = 600 keV, which corresponds to a lifetime of longer than 300 fm/c) and decays therefore far away from the reaction zone. It is therefore reasonable to consider a model with a sequential decay mechanism in the sudden approximation: a knock-out of a neutron resulting in the unstable ^{5}He nucleus decaying into an α-particle and a neutron, as illustrated in Fig. 1.

The sudden approximation, neglecting momentum transfer to the ^{5}He subsystem in

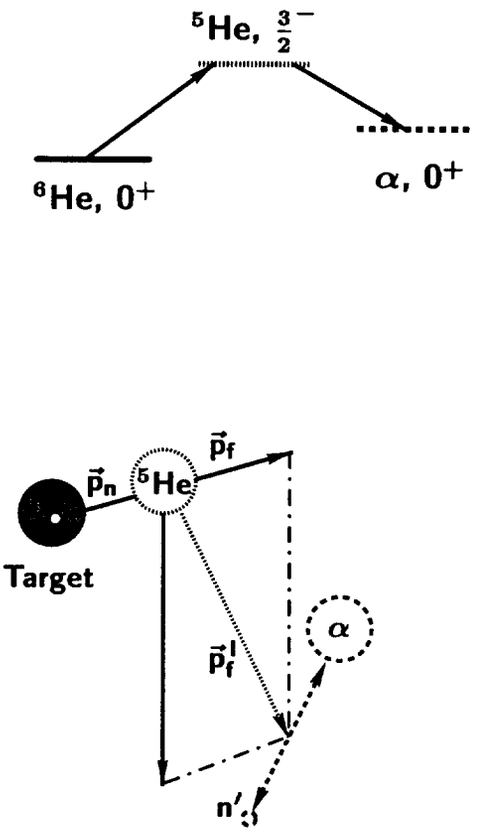

Figure 1: Schematic illustration of the fragmentation mechanism (one neutron knock-out resulting in the unbound nucleus ^{5}He). In the ^{6}He rest frame, the momentum of the ^{5}He ($\mathbf{p}_f$) is equal to the momentum of a neutron inside the projectile but has the opposite direction ($\mathbf{p}_n = -\mathbf{p}_f$). In the sudden approximation, the momentum distribution of ^{5}He in the projectile system reflects the internal momentum distribution of the removed neutron in ^{6}He. In the laboratory frame, the ^{5}He momentum, $\mathbf{p}_f^l$, is that from a Lorentz tranformation. Subsequently, the ^{5}He disintegrates into an α - paricle and a neutron n' (indicated in the ^{5}He rest frame). As indicated in the upper part of the figure, the process proceeds mainly via the 3/2− ground state of ^{5}He with a lifetime longer than 300 fm/c, thus decaying far away from the reaction zone.

the knock-out reaction, justifies the assumption that in the ^{6}He rest frame, the resulting momentum of the ^{5}He ($\mathbf{p}_f$) is equal to the momentum of the neutron knocked out from the projectile but in opposite direction ($\mathbf{p}_n = -\mathbf{p}_f$). The momentum distribution of the fragment is thus mainly determined by the internal momentum distribution of the removed neutron in the projectile, which in turn is determined by the projectile ground state wave function.

In order to describe the sequential fragmentation, ^{6}He $\rightarrow$ n+ ^{5}He $\rightarrow$ α +n, we have adopted a model based on a Monte Carlo technique. This gives a very convenient way to correct for the experimental resolution of the measured fragment momenta as well as for the limited acceptance of the experimental set-up. The latter results in asymmetric acceptance constraints of the momenta of the detected particles. The Monte-Carlo technique thus allows a straightforward comparison of a theoretical model with experimental results. The model consists of three parts:

- *Calculation of the momentum distributions of the decay products in the rest frame of ^{5}He.*

  The energy spectra of the α-particle and the neutrons in this frame can be described by a single resonance R-matrix formalism since it is assumed that the reaction mainly

proceeds via the ^{5}He ground state. The following Breit-Wigner parameterization of the resonance was used

$$\frac{d\sigma}{dE_{\alpha n}} \sim \frac{\Gamma(E_{\alpha n})}{(E_{\alpha n} - E_r)^2 + \frac{1}{4}\Gamma(E_{\alpha n})^2} \tag{1}$$

with $\Gamma(E_{\alpha n}) = 2\gamma^2 P(E_{\alpha n})$ where γ is the reduced width of the resonance and $P(E_{\alpha n})$ its penetrability. The quantity E_r is equal to $\epsilon_r + \Delta(\epsilon_r)$ where $\Delta(\epsilon_r)$ is the level shift parameter. The resonance parameters for this p-wave resonance with J^π=3/2$^-$ (E_r=0.7714 MeV, $\Gamma(\epsilon_r)$ = 0.6438 MeV, ϵ_r = 0.9631 MeV) were taken from [20].

- *The momentum distribution of the ^{5}He resonance.*

  As mentioned above, in the sudden approximation, the momentum distribution of ^{5}He in the projectile system reflects the internal momentum distribution of the removed neutron in ^{6}He, which in turn is determined by the ^{6}He ground state wave function.

  A calculation in a microscopic cluster model predicts a shape of the neutron momentum distribution in ^{6}He as being close to a Gaussian with a width σ = 73 MeV/c [11] which is shown in Fig. 2 as a solid line.

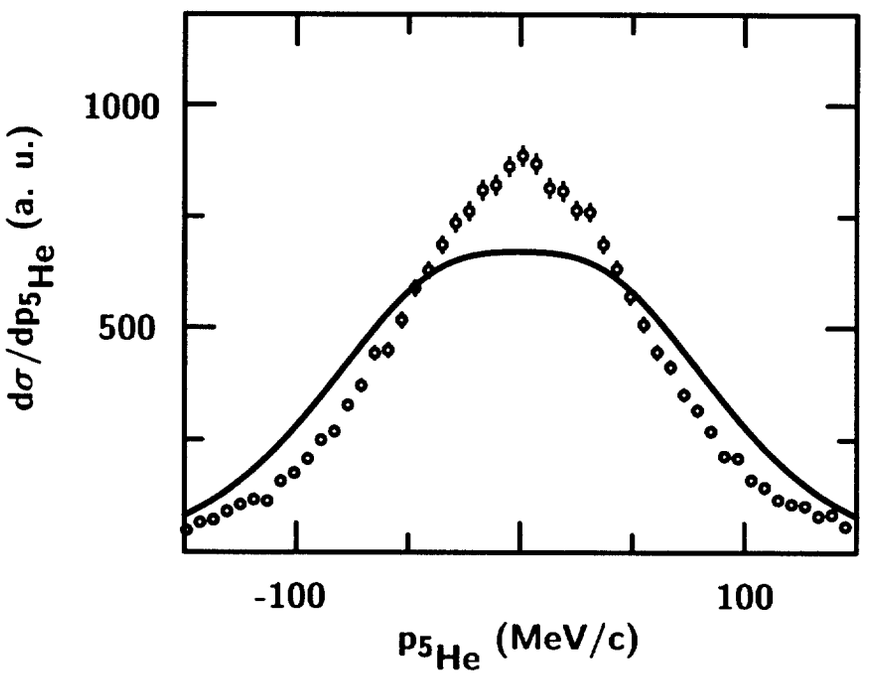

Figure 2: Distribution of ^{5}He nuclei along one transverse momentum component. The solid line represents calculations based on the Fourier transform of the ^{6}He wave function obtained [11] in the three-body model ($\alpha + n + n$). The open circles show the distribution reconstructed from the measured momenta of α- particles and neutrons ($\mathbf{p}_{^5He} = \mathbf{p}_\alpha + \mathbf{p}_n$).

It should, however, be noted that this calculation is not corrected for the peripheral nature of the process which means that the calculation was performed in the transparent limit of the Serber model. In general, instead of using a Fourier transform of the whole wave function, one has to use the Fourier transform of a cutoff portion of it. This procedure leads usually to a more narrow momentum distribution of fragments for the two-body case as shown in [21, 22]. A similar effect is expected in the case of a three-body system but such calculations are much more elaborate and not yet available.

- *Transformation of the distributions calculated in the ^{5}He rest frame to the spectator system.*

  If one assumes a sudden knock-out of a neutron from ^{6}He this also implies that there is no momentum transfer to the ^{5}He subsystem during the reaction. This leads to the conclusion that the angular distributions of the α-particles and the neutrons (as well as the ^{5}He momentum distributions) have to be isotropic in the projectile (or beam) rest frame. Such a frame is, in fact, the most convenient for theoretical estimates.

  In real experiment, however, a small momentum transfer is always present but a simple correction for this can be made. It is an accepted fact in the physics of nuclear fragmentation at high energies, that the projectile nucleons not involved in the interaction with the target (spectators) form a source for fragments. This source moves along the beam direction with a velocity slightly lower than the beam velocity and it emits fragments isotropically (see e.g. [23]). Application of this picture in our case suggests that both the detected α-particle and the neutron are spectators. We have checked that such a spectator frame, where the mean values of the neutron and α-particle velocities are equal to zero and their angular distributions are nearly isotropic, exists in our case. In this frame the ^{5}He momentum distribution is also isotropic and centered around zero. This spectator frame is moving along the beam direction with a velocity close to the beam velocity. The results of our calculations will therefore be presented in the spectator frame.

The Breit-Wigner parameterization (1) was used to generate the energies (or momenta) and angular distributions of the α-particles and neutrons in the ^{5}He rest frame. The transformation to the spectator system was made using the experimentally measured ^{5}He momentum distribution.

Monte-Carlo calculations of the α-particle and the neutron momentum distributions were performed both under the assumption of isotropic and anisotropic angular distributions between the vectors

$$\mathbf{p}_{\alpha n} = \frac{m_n m_\alpha}{m_n + m_\alpha}\left(\frac{\mathbf{p}_n}{m_n} - \frac{\mathbf{p}_\alpha}{m_\alpha}\right)$$

and

$$\mathbf{p}_{^5He} = \mathbf{p}_n + \mathbf{p}_\alpha.$$

In the case of anisotropy, we used a correlation function of the form

$$W \sim 1 + 1.5(\hat{\mathbf{p}}_{\alpha n} \cdot \hat{\mathbf{p}}_{^5He})^2,$$

where $\hat{\mathbf{p}}_{\alpha n}$ and $\hat{\mathbf{p}}_{^5He}$ are the unit vectors. This choice was obtained from experimental results presented elsewhere [24].* It was found that the momentum distributions of α-particles and neutrons and their invariant mass spectrum are insensitive to such angular correlations.

Furthermore, the experimental resolution of the α- particle and neutron momenta was taken into account in the Monte Carlo calculations. The simulated events were analysed in the same way as the experimental data.

4 Experimental results

The transverse momentum distribution of the ^{5}He fragments was reconstructed from the measured momenta of neutrons and α-particles. The data are shown in Fig. 2 together with the result of a calculation based on the microscopic cluster model [11] (solid line). The width of the experimental distribution is 61.6±0.2 MeV/c which is smaller than the calculated one, which might reflect the peripheral nature of the reaction mechanism.

Important information revealed by our data is that the mean values of the longitudinal velocities for α-particles and the neutrons are equal. This fact is directly linked to the reaction mechanism and makes it possible to introduce a spectator rest-frame system as discussed above. The velocity of this coordinate frame is about 0.5±0.1 % smaller than the experimentally determined beam velocity. This difference, however, is close to the experimental uncertainty connected to the determination of the beam velocity. The experimental uncertainty in the beam velocity thus prevents a quantitative estimate of the momentum transfer in the reaction. The difference in velocities of the coordinate systems influences only the angular distribution of the fragments. The angular distributions both for neutrons and for α-particles are nearly isotropic in the spectator rest frame as can be seen in Fig. 3a and Fig. 3b. This observation is equivalent to the statement that the fragment momentum distributions in the longitudinal and transverse directions are identical and centered at zero. The momentum distribution of their center of mass motion (^{5}He) is centered at zero and rather broad with a standard deviation of 61.6±0.2 MeV/c. The angular distribution of the ^{5}He fragments is also isotropic. These features, as we show below, favour an analysis of the fragmentation process in the spectator system.

The transverse momentum distribution of neutrons is presented in Fig. 4a. The distribution has a shape close to a Gaussian with a width $\sigma = 28.8 \pm 0.2$ MeV/c. The neutron

If we consider sudden break-up of the ^{6}He(0^+) to the n+^{5}He($3/2^-$) or n+^{5}He($1/2^-$) channels, then the correlation W will in general have a form $a + b(\hat{\mathbf{p}}_{\alpha n} \cdot \hat{\mathbf{p}}_{^5He})^2$ [25]. If the intermediate state is a pure $3/2^-$ state followed by a subsequent neutron decay to ^{4}He the calculated correlation function will have the form 0.5+1.5 $(\hat{\mathbf{p}}_{\alpha n} \cdot \hat{\mathbf{p}}_{^5He})^2$ which is more anisotropic than found in [24]. However, mixing from the ^{5}He*($1/2^-$) state would diminish the anisotropy.

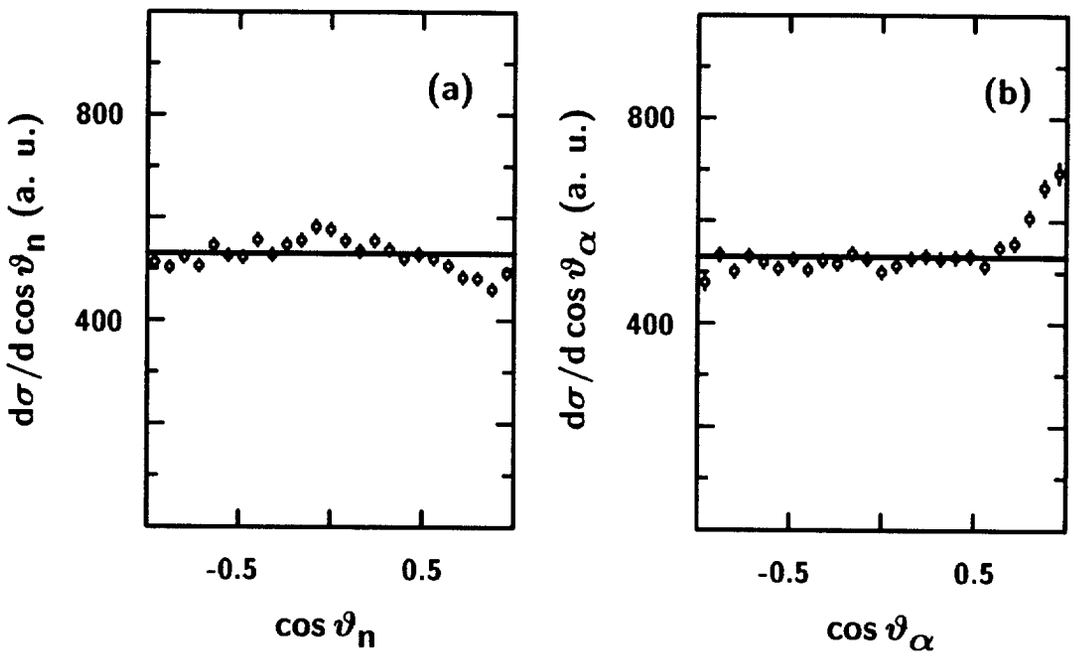

Figure 3: Distributions in polar angles of neutrons (a) and α-particles (b) in the spectator rest frame. The z-axis has been choosen along the beam direction.

momentum distribution has also been measured at 800 MeV/u [13] and was decomposed into a narrow component superimposed on a broad one. The present results agree well with those of ref. [13] at small momenta but one observes a deviation at larger values. This can be explained as caused by the geometrical acceptance for the neutron detection in our experiment which was limited in horizontal and vertical directions to ± 50 MeV/c.

The transverse momentum distribution of α-particles has a shape as demonstrated in Fig. 4b. The standard deviation of this distribution amounts to $\sigma = 56.0 \pm 0.2$ MeV/c. The corresponding inclusive distribution has been measured [12] for α-particles after fragmentation of ^{6}He at 400 MeV/u . The shape is very similar to the one obtained from our data which was obtained by selecting coincidences between α-particles and neutrons in the forward direction.

In the next step, we use the experimentally measured momentum distribution of the ^{5}He fragments as an input in the sequential fragmentation model presented above and calculate the momentum distributions of neutrons and α-particles. The resemblance with the experimental data is excellent as shown in Fig. 4a and Fig. 4b.

However, an attempt to get evidence for an $\alpha - n$ interaction directly from the measured momentum distributions fails. The root mean square (r.m.s.) values of neutron and α-particle momenta contain in principle information about correlations. The measured r.m.s. values of the transverse momentum are:

$$\begin{aligned} < p_\alpha^2 >^{1/2} &= 56.0 \pm 0.2 MeV/c \\ < p_n^2 >^{1/2} &= 25.8 \pm 0.1 MeV/c^\dagger \end{aligned}$$

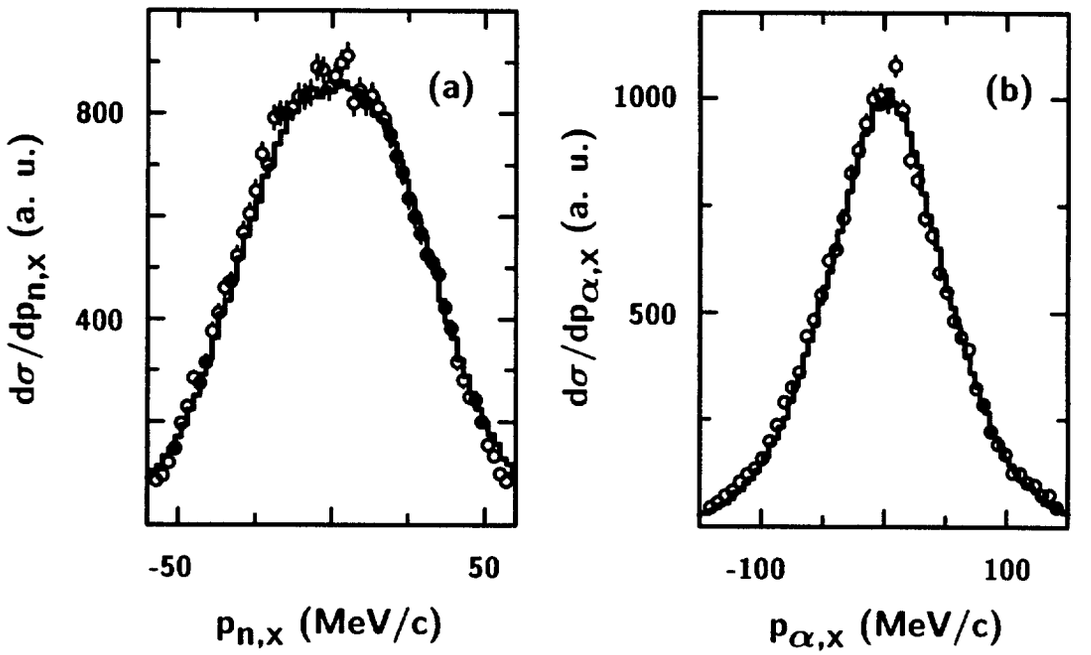

Figure 4: Distributions of neutrons (a) and α-particles (b) in one transverse momentum component p_x.The experimental data are shown by circles. The histograms are the result of Monte-Carlo calculations based on the assumption that the dominant reaction mechanism originates in one neutron knock-out resulting in the unbound nucleus ^{5}He. A Breit-Wigner parameterization of the ^{5}He $(3/2^-)$ resonance was used for the energy distribution of α-particles and neutrons in the ^{5}He rest frame, while the distribution of ^{5}He momenta was taken from the experimental data shown in Fig. 2.

$$< p^2_{^5He} >^{1/2} \;=\; 61.6 \pm 0.2 MeV/c$$

The ^{5}He r.m.s. momentum is almost exactly equal to $\sqrt{< p^2_\alpha > + < p^2_n >} = 61.7$ MeV/c indicating that the term $< p_\alpha p_n >$ is close to zero. The r.m.s. momenta thus show no evidence for an $\alpha - n$ interaction. Partially, this insensitivity is connected to the limited acceptance of the experimental set-up. The main reason is, however, the randomly oriented distribution of the ^{5}He momenta. The transformation from the ^{5}He rest frame to the spectator system influences mainly the directions of α-particles (in the ^{5}He rest frame velocities of α-particles v_α are much smaller than those of neutrons, $v_\alpha = v_n/4$).

Note, that we have already seen in our calculations that the α-particle and neutron-momentum distributions do not depend on the anisotropy $(\hat{\mathbf{p}}_{\alpha n} \cdot \hat{\mathbf{p}}_{^5He})^2$.

One may expect that a strong final-state interaction corresponding to the ^{5}He ground-state resonance should clearly be observable in the invariant mass spectrum. The experimental data on the distribution of relative kinetic energy between the α - particle and the

[†]A small difference between this number and σ from the Gaussian fit is mainly connected with the limited acceptance for detection of the neutrons.

neutron is calculated from

$$E_{\alpha n} = \frac{m_\alpha + m_n}{2m_\alpha m_n}\mathbf{p}^2_{\alpha n}$$

and is shown in Fig. 5a. Indeed, a peak at an energy close to the known ^{5}He ground state resonance is seen in the experimental spectrum. The dashed line presents the theoretical invariant mass spectrum for an ideal set-up with perfect resolution and full acceptance. The experimental resolution and the limited acceptance of the detector result in a wider distribution which is displayed in Fig. 5a by a histogram. Good agreement of the calculation with experimental data was obtained except for very low energies ($E_{\alpha n}$< 0.5 MeV) where the experimental cross section is larger.

The simple model of sequential fragmentation of ^{6}He is thus very successful in describing the measured momentum distributions, as well as the invariant mass spectra. It should, however, be pointed out that nothing has been assumed about background structures in the invariant mass spectra that have their origin in the reaction mechanism, but not in resonances in the subsystems.

If the reaction proceeds via a resonance, a peak will appear in the invariant mass distribution on top of a possible background mentioned above. In some cases, especially in fragmentation reactions, the background may, however, also reveal a peak-like structure. The relative energy distributions of the fragments reflect the internal motion of fragments inside the projectile [26, 27], and the probability of a large relative energy E_{rel} is therefore rapidly decreasing towards higher energy, especially for loosely bound halo nuclei. On the other hand the spectral shape at low energies in fragmentation processes is determined by phase space and is proportional to $E_{rel}^{l+1/2}$, where l is the relative angular momentum of the fragments. Therefore, it is expected that a peak-like background structure could be observed in any invariant mass spectrum, which may shift the resonance or change its shape. In the worst case such a background may be interpreted as a resonance, even if there are no correlations. Another important fact is the limited acceptance of the detectors as this may create an artificial structure in the invariant mass distribution.

5 Correlation function

The only way to get real evidence for correlations between the fragments and to eliminate the background contributions and effects due to finite detector acceptance is to construct an appropriate correlation function. For this purpose, we first need to construct a randomised spectrum ($dN^{ran}/dE_{\alpha n}$) which will be calculated from the inclusive spectra of neutrons and α-particles according to

$$\frac{dN^{ran}}{dE_{\alpha n}} = \frac{1}{N}\left[\int \frac{d^3N}{d\mathbf{p'}_\alpha}\frac{d^3N}{d\mathbf{p'}_n}\delta(E_{\alpha n} - E'_{\alpha n})d\mathbf{p'}_\alpha d\mathbf{p'}_n\right];$$

where N is the number of events. To solve the integral in practice, we use an event mixing procedure where a randomised relative energy $E_{\alpha n}$ is obtained by combining α-particle

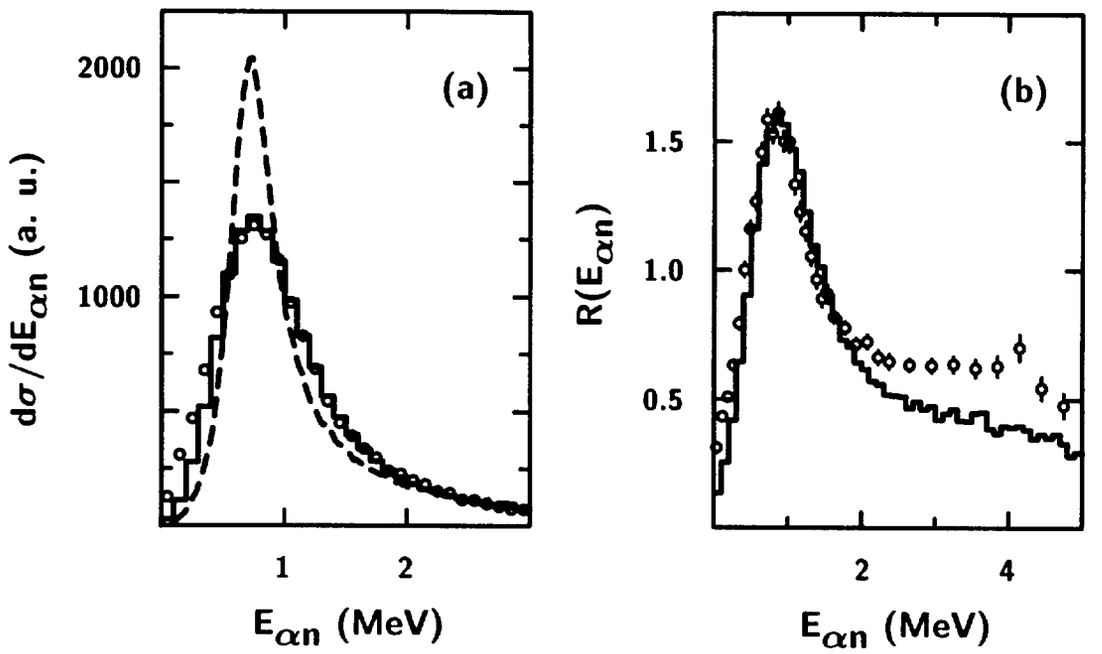

Figure 5: (a) - Relative kinetic energy distribution of the $\alpha - n$ system (invariant mass spectrum). The experimental data are shown as circles. The dashed line displays a parameterization of the resonance by a Breit-Wigner expression (Eq.1) (see explanation in the text). The histogram is the result of the calculations for the sequential fragmentation model (see Section 3) where the experimental resolution and effects due to the finite acceptance are taken into account.
(b) - Correlation functions obtained by an event mixing method. The open circles show the experimental correlation function which is obtained from the experimental invariant mass spectrum (shown in Fig. 5a) divided by the randomised spectrum. The histogram represents the correlation function obtained from the sequential fragmentation model.

and neutron momentum vectors taken from different events. Such a procedure will wash out all possible correlations in the randomised spectrum and the integration over angles is then automatically confined to momentum vectors within the detector acceptance. The correlation function is then defined as the ratio of the invariant mass spectrum and the randomised one

$$R(E_{\alpha n}) = \frac{dN/dE_{\alpha n}}{dN^{ran}/dE_{\alpha n}}. \tag{2}$$

This method removes the artificial structure in the invariant mass distributions coming from the finite acceptance of the detectors. The correlation function determined in this way is equal to one if the distribution of the relative angle between fragments is isotropic and the energy of one fragment does not depend on the energy of the second fragment. The correlation function does not depend on the shapes of neutron and α-particle spectra,

but deviates from unity if there are correlations between the angles and energies of the two particles.

The quantity $R(E_{\alpha n})$ should indicate effects of correlations and the location in energy where such correlations become most pronounced. The two-particle resonance has to result in a peak in the correlation function with a position close to the position of the peak in the invariant mass spectrum.

This type of correlation functions has often been used in the analysis of elementary particle physics experiments to estimate a background in the invariant mass spectra of particles which may be decay products of resonances (e.g. [28, 29, 30]). It was as well used for the search of two-particle resonances in the fragmentation of heavy nuclei [31].

Both the theoretical and experimental correlation functions were obtained as described above by the event mixing procedure and are shown in Fig. 5b.

The theoretical, as well as the experimental correlation function reveal distinct deviations from unity and have peak positions close to the known energy of the ^{5}He ground state. The good agreement obtained between the calculation and the experimental data indicates that we have an almost pure case of a ^{5}He (=α+n) resonance. The uncorrelated background, as well as possible effects due to correlations between the neutrons and α-particle coming from the three-body ^{6}He wave function, do not give a significant contribution neither to the invariant mass spectra nor to the correlation function up to an energy of 2 MeV.

6 Summary

The experimental data on momentum distributions of α-particles and neutrons and the invariant mass spectra obtained from fragmentation of a 240 MeV/u ^{6}He beam on a carbon target have been presented.

The sequential fragmentation model with a sudden knock-out of a neutron leading to a particle unstable ^{5}He (J^π=3/2$^-$) resonance, i.e. the ^{5}He ground state, can reproduce the measured momentum distributions as well as the invariant mass spectrum of the $n-\alpha$ system. Nevertheless, two-body correlations between the α-particle and the neutron are not evident in such distributions. The widths of the fragment momentum distributions are not very sensitive to the correlations between fragments. It was, however, shown that the simultaneous analysis of the invariant mass spectrum and the correlation function can unambiguously give an indication for correlations between the reaction products.

All results together indicate that in the two-particle channel of ^{6}He fragmentation on a carbon target, there is not much space left for the appearance of the projectile structure. The momentum distributions for both neutrons and α-particles and their invariant mass spectrum and correlation function are strongly influenced by the ^{5}He ground state resonance. The only place where one may expect effects due to the ^{6}He structure is the ^{5}He momentum distribution itself. This should be studied in the fragmentation of ^{6}He on a heavy target where Coulomb dissociation makes a significant contribution and in the

reaction channel where both neutrons and the α-particle are observed in coincidence.

This work was supported by the German Federal Minister for Education and Research (BMBF) under Contracts 06 DA 820, 06 OF 474 and 06 MZ 476 and by GSI via Hochschulzusammenarbeitsvereinbarungen under Contracts DARIK, OF ELK, MZ KRK and partly supported by the Polish Committee of Scientific Research under Contract PB2/P03B/113/09, EC under Contract ERBCHGE-CT92-0003 and CICYT under Contract AEN92-0788-C02-02 (MJGB) and by Deutsche Forschungsgemeinschaft (DFG) under Contract 436 RUS 130/127/1. One of us (B.J.) acknowledges the support through an Alexander von Humboldt Research Award.

References

[1] P.G. Hansen, A.S. Jensen and B. Jonson, Ann. Rev. Nucl. Part. Sci. **45** (1995) 591

[2] I. Tanihata, J. Phys. (London) **G22** (1996) 157

[3] M.V. Zhukov, B.V. Danilin, D.V. Fedorov, J.M. Bang, I.J. Thompson and J.S. Vaagen, Phys. Rep. **211** (1993) 151

[4] M.J.G. Borge, P.G. Hansen, L. Johannsen, B. Jonson, T. Nilsson, G. Nyman, A. Richter, K. Riisager, O. Tengblad, K. Wilhelmsen and the ISOLDE Collaboration, Z. Phys. **A340** (1991) 255

[5] I. Tanihata, D. Hirata, T. Kobayashi, S. Shimoura, K. Sugimoto and H. Toki, Phys. Lett. **289B** (1992) 261

[6] V.I. Kukulin, V.T. Voronchev, T.D. Kaipov and R.A. Eramzhyan, Nucl. Phys. **A517** (1990) 221

[7] B.V. Danilin, M.V. Zhukov, A.A. Korsheninnikov and L.V. Chulkov, Yad. Fiz. **53** (1991) 71; Sov. J. Nucl. Phys. **53** (1991) 45

[8] Y. Suzuki, Nucl. Phys. **A528** (1991) 395,
K. Varga, Y. Suzuki and Y. Ohbayasi, Phys. Rev. **C50** (1994) 189

[9] A. Csótó, Phys. Rev. **48** (1993) 165

[10] S. Funada, H. Kameyama and Y. Sakuragi, Nucl. Phys. **A575** (1994) 93

[11] M.V. Zhukov, L.V. Chulkov, B.V. Danilin and A.A. Korsheninnikov, Nucl. Phys. **A533** (1991) 428

[12] T. Kobayashi, Nucl. Phys. **A538** (1992) 343c

[13] T. Kobayashi, Nucl. Phys. **A553** (1993) 465c

[14] A.A. Korsheninnikov and T. Kobayashi, Nucl. Phys. **A567** (1994) 97

[15] H. Geissel, P. Armbruster, K.H. Behr, A. Brünle, K. Burkard, M. Chen, H. Fogler, B. Franczak, H. Keller, O. Klepper, B. Langenbeck, F. Nickel, E. Pfeng, M. Pfützner, E. Roeckl, K. Rykaczewski, I. Schall, D. Schardt, C. Scheidenberger, K.-H. Schmidt, A. Schröter, W. Schwab, K. Sümmerer, M. Weber, G. Münzenberg, T. Brohm, H.-G. Clerc, M. Fauerbach, J.-J. Gaimard, A. Grewe, E. Hanelt, B. Knödler, M. Steiner, B. Voss, J. Weckenmann, C. Ziegler, A. Magel, H. Wollnik, J.P. Dufour, Y. Fujita, D.J. Viera and B. Sherrill, Nucl. Instr. and Meth. in Phys. Research **B70** (1992) 286.

[16] T. Nilsson, F. Humbert, W. Schwab, H. Simon, M.H. Smedberg, M. Zinser, Th. Blaich, M.J.G. Borge, L.V. Chulkov, Th.W. Elze, H. Emling, H. Geissel, K. Grimm, D. Guillemaud-Mueller, P.G. Hansen, R. Holzmann, H. Irnich, B. Jonson, J.G. Keller, H. Klinger, A.A. Korsheninnikov, J.V. Kratz, R. Kulessa, D. Lambrecht, Y. Leifels, A. Magel, M. Mohar, A.C. Mueller, G. Münzenberg, F. Nickel, G. Nyman, A. Richter, K. Riisager, C. Scheidenberger, G. Schrieder, B.M. Sherrill, K. Stelzer, J. Stroth, O. Tengblad, W. Trautmann, E. Wajda, M.V. Zhukov and E. Zude, Nucl. Phys. **A598** (1996) 418

[17] M. Zinser, F. Humbert, T. Nilsson, W. Schwab, H. Simon, T. Aumann, M.J.G. Borge, L.V. Chulkov, J. Cub, Th.W. Elze, H. Emling, H. Geissel, D. Guillemaud-Mueller, P.G. Hansen, R. Holzmann, H. Irnich, B. Jonson, J.V. Kratz, R. Kulessa, Y. Leifels, H. Lenske, A. Magel, M. Mohar, A.C. Mueller, G. Münzenberg, F. Nickel, G. Nyman, A. Richter, K. Riisager, C. Scheidenberger, G. Schrieder, K. Stelzer, J. Stroth, A. Surowiec, O. Tengblad, E. Wajda and E. Zude, Nucl. Phys. **A619** (1997) 151

[18] LAND Collaboration, Th. Blaich, Th.W. Elze, H. Emling, H. Freiesleben, K. Grimm, W. Henning, R. Holzmann, G. Ickert, J.G. Keller, H. Klingler, W. Kneissl, R. König, R. Kulessa, J.V. Kratz, D. Lambrecht, J.S. Lange, Y. Leifels, E. Lubkiewicz, M. Proft, W. Prokopowicz, C. Schütter, R. Schmidt, H. Spies, K. Stelzer, J. Stroth, W. Walus, E. Wajda, H.-J. Wollersheim, M. Zinser and E. Zude, Nucl. Instr. and Meth. in Phys. Research, **A314** (1992) 136

[19] E. Garrido, D.V. Fedorov and A.S. Jensen, Nucl. Phys. **A617** (1997) 153

[20] J.E. Bond and F.W.K. Firk, Nucl. Phys. **A287** (1977) 317

[21] P.G. Hansen, Phys. Rev. Lett **77** (1996) 1016

[22] H. Esbensen, Phys. Rev. **C53** (1996) 2007

[23] W.G. Lynch, Ann. Rev. Nucl. Part. Sci. **37** (1987) 493

[24] L.V. Chulkov, T. Aumann, D. Aleksandrov, L. Axelsson, T. Baumann, M.J.G. Borge, R. Collatz, J. Cub, W. Dostal, B. Eberlein, Th.W. Elze, H. Emling, H. Geissel, V.Z. Goldberg, M. Golovkov, A. Grünschloß, M. Hellström, J. Holeczek, R. Holzmann, B. Jonson, A.A. Korsheninnikov, J.V. Kratz, G. Kraus, R. Kulessa, Y. Leifels, A. Leistenschneider, T. Leth, I. Mukha, G. Münzenberg, F. Nickel, T. Nilsson, G. Nyman, B. Petersen, M. Pfützner, A. Richter, K. Riisager, C. Scheidenberger, G. Schrieder, W. Schwab, H. Simon, M.H. Smedberg, M. Steiner, J. Stroth, A. Surowiec, T. Suzuki and O. Tengblad, Phys. Rev. Lett. **79** (1997) 201.

[25] L.C. Biedenharn and M.E. Rose, Rev. Mod. Phys. **25** (1953) 729

[26] A.S. Goldhaber, Phys. Lett. **53B** (1974) 306

[27] W.A. Friedman, Phys. Rev. **C27** (1983) 569

[28] E.L. Berger, R. Singer, G.H. Thomas and T. Kafka, Phys. Rev. **D15** (1977) 206

[29] G. Jancso, M.G. Albrow, S. Almehed, P.S.L. Booth, X. De Bouard, J. Burger, H. Bøggild, L.J. Carroll, P. Catz, E. Dahl-Jensen, I. Dahl-Jensen, G. Damgaard, G. von Dardel, N. Elverhaug, B. Guillerminet, K. Hansen, P. Herbsleb, J.N. Jackson, G. Jarlskog, H.B. Jensen, L. Jönsson, A. Klovning, E. Lillethun, R. Little, E. Lohse, A. Lu, B. Lörstad, N.A. McCubbin, A. Melin, H.E. Miettinen, J.V. Morris, R. Møller, S.Ø. Nielsen, B.S. Nielsen, J.O. Petersen, T. Sanford, J.A.J. Skard, D.B. Smith and P. Villeneuve, Nucl. Phys. **B124** (1977) 1

[30] D. Drijard, H.G. Fischer and T. Nakada, Nucl. Instr. and Meth. in Phys. Research, **225** (1984) 367

[31] J. Pochodzalla, C.K. Gelbke, W.G. Lynch, M. Maier, D. Ardouin, H. Delagrange, H. Doubre, C. Grégoire, A. Kyanowski, W. Mittig, A. Péghaire, J. Péter, F. Saint-Laurent, B. Zwieglinski, G. Bizard, F. Lefebvres, B. Tamain, J. Québert, Y.P. Viyogi, W.A. Friedman and D.H. Boal, Phys. Rev. **C35** (1987) 1695